crystals

MDPI

Article

Experiment and Numerical Simulation on Friction Ignition Response of HMX-Based Cast PBX Explosive

Junming Yuan [1,*], Yue Qin [1], Hongzheng Peng [2], Tao Xia [1], Jiayao Liu [1,2], Wei Zhao [2], Hu Sun [1] and Yan Liu [1]

[1] School of Environment and Safety Engineering, North University of China, Taiyuan 030051, China; s202114014@st.nuc.edu.cn (Y.Q.); s2014028@st.nuc.edu.cn (T.X.); s2014038@st.nuc.edu.cn (J.L.); sz202114018@st.nuc.edu.cn (H.S.); sz202114036@st.nuc.edu.cn (Y.L.)

[2] Chongqing Hongyu Precision Industry Group Co., Ltd., Chongqing 402760, China; wll@hongyu.com (H.P.); hty@hongyu.com (W.Z.)

* Correspondence: yuanjm@nuc.edu.cn

Abstract: In order to study the ignition process and response characteristics of cast polymer-bonded explosives (PBX) under the action of friction, HMX-based cast PBX explosives were used to carry out friction ignition experiments at a 90° swing angle and obtain the critical ignition loading pressure was 3.7 MPa. Combined with the morphology characterization results of HMX-based cast PBX, the friction temperature rise process was numerically simulated at the macro and micro scale, and the ignition characteristics were judged. The accuracy of the numerical simulation results was ensured based on the experiment. Based on the thermal–mechanical coupling algorithm, the mechanical–thermal response of HMX-based cast PBX tablet under friction was analyzed from the macro scale. The results show that the maximum temperature rise is 55 °C, and the temperature rise of the whole tablet is not enough to ignite the explosive. Based on the random circle and morphology characterization results of tablet, the mesoscopic model of HMX-based cast PBX was constructed, and the microcrack friction formed after interface debonding was introduced into the model. The temperature rise process at the micro scale shows that HMX crystal particles can be ignited at a temperature of 619 K under 4 MPa hydraulic pressure loaded by friction sensitivity instrument. The main reason for friction ignition of HMX-based cast PBX is the friction hot spot generated by microcracks formed after interface damage of the tablet mesoscopic model, and the external friction heat between cast PBX tablet and sliding column has little effect on ignition. External friction affects the ignition of HMX-based cast PBX by influencing the formation of internal cracks and the stress at microcracks.

Keywords: numerical simulation; friction sensitivity; ignition; cast PBX; mesoscopic model

Citation: Yuan, J.; Qin, Y.; Peng, H.; Xia, T.; Liu, J.; Zhao, W.; Sun, H.; Liu, Y. Experiment and Numerical Simulation on Friction Ignition Response of HMX-Based Cast PBX Explosive. *Crystals* **2023**, *13*, 671. https://doi.org/10.3390/cryst13040671

Academic Editors: Rui Liu, Yushi Wen and Weiqiang Pang

Received: 15 March 2023
Revised: 3 April 2023
Accepted: 7 April 2023
Published: 13 April 2023

1. Introduction

Cast PBX is a kind of high polymer-bonded explosive, which is widely used in high-speed penetration and damage weapons because of its good mechanical properties and low sensitivity. During the transportation, storage and use of casting PBX charge warheads, accidental ignition may occur due to external stimulation, which greatly affects the reliability and safety of weapons. Friction is one of the important stimulation sources. A lot of experiments and numerical simulations have been done on the ignition of explosives under friction. Min-cheol Gwak et al. [1] analyzed the friction ignition process of HTPB based solid propellant from the perspectives of reaction kinetics and friction heating, and built relevant models to predict the ignition time of propellant under friction action through numerical simulation. Sun Baoping et al. [2] carried out numerical simulation of PBX tablet friction-ignition experiment based on the finite element method, and analyzed the influence of pressure, velocity, and friction coefficient on ignition. Deng Chuan et al. [3] established a test method for friction sensitivity of pendulum impact-driven sand target friction explosive tablets, and tested the friction sensitivity of three PBX tablets. R. Charley et al. [4] studied the friction ignition process of solid propellant based on friction device, which

can obtain the overall deformation process of propellant by high-speed photography, and then simulate the response of solid propellant under friction by discrete element method. And compare the cloud image of numerical simulation with the topography of high-speed photography. The deformation process analyzed by the discrete element method is in good agreement with the actual deformation process and can reflect the meso-ignition process of the explosive. Dai Xiaogan et al. [5] carried out the friction ignition experiment on PBX and designed a device to calculate the friction work and friction power threshold of explosive ignition under friction and analyzed the ignition mechanism of explosive in the friction sensitivity experiment. The results show that it is difficult to heat PBX as a whole and make it ignite under friction. Zeman et al. [6] provided an overview of the main developments over the past nine years in the study of the sensitivity of energetic materials (EM) to impact, shock, friction, electric spark, laser beams and heat. Luo Yi et al. [7] and others carried out slide experiment and Numerical Simulation Research on PBX-8701, and analyzed the influence of external-friction coefficient on ignition delay time based on the theory of heat transfer and diffusion and reaction kinetics.

The ignition phenomenon of explosives under external stimulation can be explained by the hot spot theory. Dienes et al. [8] analyzed and compared four hot spot mechanisms (pore collapse; hole collapse; hole collapse) in the projectile target experiment, shock heating, shear band under plastic flow. The results show that the interface friction of closed crack is the main reason of hot spot. Randolph et al. [9] developed a friction ignition model to predict the thermal decomposition of condensed phase explosives when impacted at an oblique angle on a rigid target surface. Andersen et al. [10] established a mathematical relationship between the friction coefficient of materials and the parameters that affect friction during shearing. An et al. [11] used the ReaxFF force field to study the hot spot formation mechanism of PBXN-106 explosive under the action of shock waves. The shear relaxation of the micro-convex body at the interface of the density discontinuity caused by the impact resulted in energy deposition, and the local shear in this region formed a hot spot, which was eventually accompanied by chemical reactions leading to the explosion of the system. It is concluded that reducing the density of the binder (about 1/3 of the explosive density) can inhibit the hot spot generation. Cai et al. [12] used molecular dynamics to simulate the impact response characteristics of coarse-grained explosives and pointed out that both interparticle friction and shear deformation between particles can generate hot spots, and the direction of shear slip between particles significantly affects the frictional heat generation efficiency. Keshavarz et al. [13] presented a novel general simple model for prediction of the relationship between friction sensitivity and activation energy of thermolysis of cyclic and acyclic nitramines on the basis of their molecular structures. Richard et al. [14] studied the response to mechanical non-shock stimulation using explosive-driven deformation test and ballistic impact chamber. According to the experimental results, the shear rate threshold as a single parameter to describe the mechanical sensitivity is challenged, and preference is given to the development of an ignition criterion based on intergranular sliding friction under the action of a normal pressure. Hu et al. [15] presented a combined computational–experimental study of the mesoscale thermo-mechanical behavior of HTPB bonded AP composite energetic material subjected to dynamic loading conditions. The computational model considers the AP-HTPB interface debonding, post debonding interface friction and temperature rise due to viscoelastic dissipation as well as dissipative interfacial processes. Jafari et al. [16] introduced a reliable method to predict friction sensitivity of quaternary ammonium-based EILs, which are based on elemental composition of cation and anion of a desired ionic liquid as well as the contribution of specific cations and anions. Gruau et al. [17] simulated the behavior of the PBX by means of the elastic-plastic damage law and the ignition criterion due to localization of plastic strain in the microstructure, and the simulation results were consistent with the experimental results. Wu et al. [18] developed a micromechanical ignition model of the hot spot formation of HMX and PETN mixed powder explosives under the impact of a falling hammer in the fine structure, estimated the temperature rise caused by plasticity and frictional dissipation, and added the self-heating

reaction model of explosives to predict the hot spot ignition by thermal explosion. Joel G. Bennett et al. [19] proposed visco elastic statistical crack ignition model (visco-scram) for numerical simulation of non-shock ignition of PBX explosives. In this model, the friction heat of microcracks is taken as the main source of hot spot formation, and the mechanical behavior of PBX explosives is considered. As a classical non-shock ignition model, this model is widely used. However, there are many parameters in the model, and it is difficult to calibrate. For different explosive formulations, it is necessary to re determine the material parameters, so the pretreatment process of numerical simulation is relatively complex. Xue, H.J. et al. [20] established an improved combined microcrack and microvoid model (CMM) to study the damage and ignition behaviors of polymer-bonded explosive (PBX) under coupled impact and high-temperature loading conditions. Bai, Z.X., Li, H.T., Yin, Y. and Duarte, C.A. [21–24] have studied the friction behavior and hot spot formation of HMX explosive crystals, as well as the ignition and combustion behavior under hot spot conditions.

The research on friction ignition has gradually changed from macro to micro hot spot formation. Barua et al. [25–28] studied the temperature rise process of PBX9501 from micro scale by CFEM finite element method. Based on the digital image processing technology, a mesoscopic model was established, which was consistent with the actual situation. The friction heating of microcracks caused by the failure of the interface between particles and matrix was studied. The relationship between the particle-failure mechanism and the overall temperature rise of PBX has been researched. Amirreza Keyhani et al. [29] analyzed the ignition process of PBX9501 at meso level based on CFEM method and considered the contribution of friction and viscoelastic plastic dissipation energy of microcracks formed after damage to temperature rise. The research results show that the viscoelastic plastic dissipation energy has little effect, and the energy contributed by crack friction is the main reason for hotspot formation.

At present, there are many research studies on the ignition of pressed PBX, but relatively few studies on cast PBX, and the research on the micro ignition focuses on the impact overload, while studies on the friction overload are fewer. Therefore, HMX-based cast PBX samples were prepared and the friction-ignition experiment of cast PBX at a 90° swing angle were carried out in this paper. Based on the experimental results combined with the macro numerical simulation, the friction-ignition process and response characteristics of HMX-based cast PBX tablets are studied at the micro level, and the accuracy of the numerical simulation results is judged by friction ignition experiments.

2. Materials and Methods

2.1. Experiment

2.1.1. Preparation and Characterization of HMX-Based Cast PBX Sample

According to the typical HTPB casting PBX formulation, a small amount of casting PBX explosive samples were prepared. Cast PBX is composed of Al powder, HTPB bonding system and HMX crystal particles. All raw materials should be fully dried before preparation, and their water content must be strictly controlled. Aluminum powder and binder are thoroughly mixed and added to the main explosive in batches under heated conditions. After mixing evenly, the material is poured into the mold so that the explosive is cured at a constant temperature of 60 °C for 72 h. The formulation of cast PBX is shown in Table 1 referred from [30].

Table 1. Formulation of HMX-based cast PBX explosive.

Sample	HMX	Al	HTPB	DOA	TDI
Mass fraction	55%	33%	6%	5.8%	0.2%

Figure 1 shows the cast PBX tablets and the electron microscopic morphology. After the preparation for the cast PBX is completed, slice work is carried out, and the slice size

is about Φ10 mm × 1 mm. Because the formulation contains Al powder, the color of the tablet is grey, as shown in Figure 1a,b. The tablet was characterized by scanning electron microscope, and HMX crystal particles with a particle size range of 10~80 μm are shown in Figure 1c. The electron microscope morphology provides experimental support for the establishment of the mesoscopic model in the next friction ignition simulation.

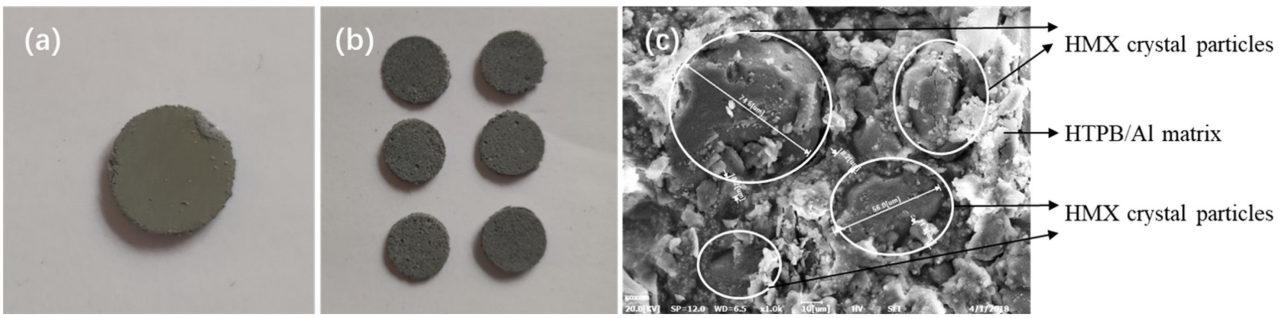

Figure 1. (**a**,**b**) HMX-based Cast PBX tablets; and (**c**) 1000 times electron microscope morphology of HMX-based PBX explosive sample.

The photographs in Figure 1c indicate the presence of micropores in cast PBX near the HMX particles and the binder matrix. This is also reflected in Figure 1b, where pores are visible on the surface of the poured PBX tablet. The binder curing process itself has pores, as shown in Figure 2a. Cast PBX tablets without vacuum pumping and uneven mixing can cause pores. The presence of pores weakens the cohesive strength of the interface boundaries and contributes to the development of deformation localization and local heating at the boundaries of HMX particles under the action of stresses arising from friction of the samples. Figure 2c shows the microstructure of HMX-based cast PBX tablets. The picture clearly shows that the HTPB/Al matrix composed of Al powder particles and adhesive is tightly wrapped with many HMX crystal particles of different sizes, providing theoretical support for the construction of a simplified model.

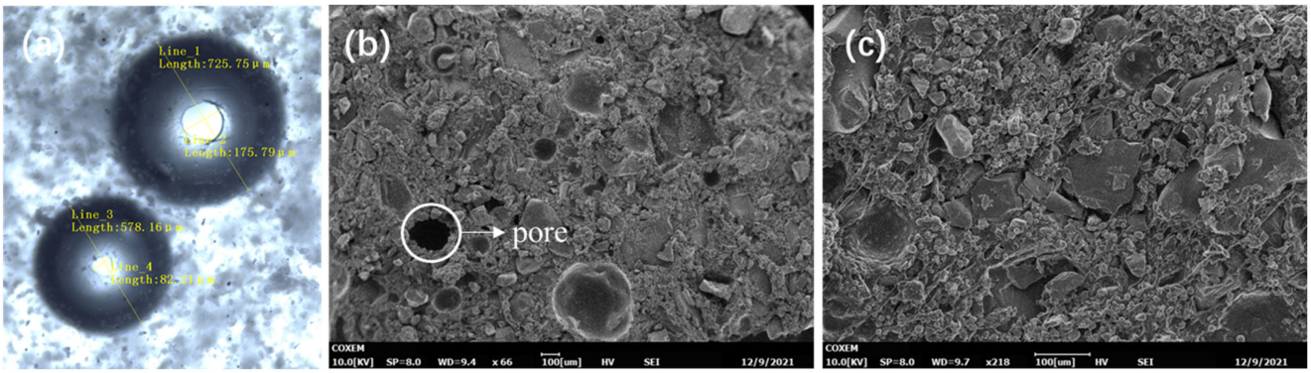

Figure 2. (**a**) HTPB binder curing pores; (**b**) Pore of HMX-based cast PBX tablets; (**c**) 200 times electron microscope morphology of HMX-based PBX explosive sample.

2.1.2. Test Process of Friction Sensitivity Experiment

The cast PBX tablet is loaded onto the sliding column end face of the friction device, and the upper sliding column is gently placed. The upper slide column is rotated for 1–2 cycles to evenly distribute the explosive sample between the end faces of the two slide columns. The loaded friction device is placed in the combustion equipment of the friction sensitivity instrument, at a 90° swing angle, and the gauge pressure raised to 4.0 MPa (or other different loading pressures). The pendulum is released, and the striking rod is struck. The striking rod causes the upper and lower sliding columns to move at high speed, causing sliding friction on the end faces of the upper and lower columns, resulting in intense friction

on the test sample. After completing this operation process, the experimenter repeats the process to perform the test on the next sample.

2.1.3. Critical Ignition Loading Pressure

MGY-I friction sensitivity instrument is used to test the friction ignition of cast PBX [31]. In order to obtain the exact critical initiation conditions of friction, the Bruceton method [32] is used for reference to the high impact sensitivity characteristics. In the test of friction sensitivity, there are two variables controllable, one is the pendulum angle and the other is the loading pressure of hydraulic press. Considering the feasibility of numerical simulation, the paper uses the loading pressure as a variable. The Bruceton method is used to determine the critical ignition loading pressure of friction sensitivity. The method is calculated according to the following formula.

$$\sigma_{50}^{f} = \left[A + B\left(\frac{C}{D} \pm \frac{1}{2} \right) \right] \tag{1}$$

$$C = \sum i \times n_i \tag{2}$$

$$D = \sum n_i \tag{3}$$

In the formula, σ_{50}^{f} is the critical ignition loading pressure of explosives; A is the minimum hydraulic pressure loaded by friction sensitivity instrument for initiation; B is the set loading pressure interval, 0.5 MPa in this paper; i is the height serial number; n_i is the sum of the number of explosion times under the height of serial number i. The friction ignition experiment was carried out under a swing angle of 90° on cast PBX tablets with the same specification. In this experiment, the loading pressure range is 2 MPa~4 MPa, and the pressure gradient is 0.5 MPa; So, A = 2 MPa, B = 0.5 MPa. Finally, the critical ignition loading pressure calculated is σ_{50}^{f} = 3.7 MPa. The calculation parameters in Formula (1) are shown in Table 2.

Table 2. Sorting of test results.

i	n_i	C/MPa	D/MPa
1	0		
2	1		
3	3	47	12
4	4		
5	4		

2.1.4. Solution of Relative Slip Rate

In order to obtain the slip rate of friction ignition experiment, the traditional friction sensitivity instrument was improved, as shown in Figure 3. A force sensor is added at the end of the striking bar. The impact force and action time of the sliding column can be measured by the force sensor, and the displacement curve of the sliding column can be obtained by the motion equation.

When measuring the friction sensitivity, the upper sliding column starts to slide to the right under the action of pendulum. The sliding speed of the upper column is not uniform. According to the F-T curve measured by the sensor, the displacement x-t curve of the sliding column can be obtained by calculating the F-T integral. The impact force F obtained does not provide acceleration for the upper sliding column, but also overcomes friction resistance F.

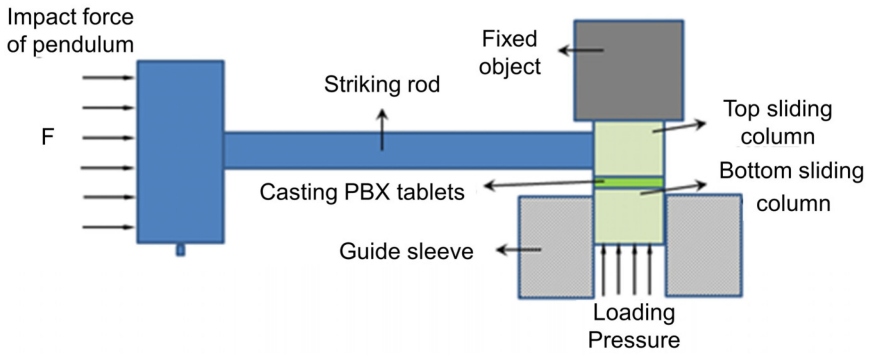

Figure 3. Pendulum impact force test device.

The velocity curve of the sliding column can be used as the boundary condition of the numerical simulation to ensure that the numerical simulation is consistent with the experiment. The slip rate curves under different loading pressures are shown in Figure 4a. Over time, under different loading pressures, the slip rate of the upper sliding column first rises and then gradually stabilizes. Under a loading pressure of 2 MPa, the slip rate curve and displacement curve are shown in Figure 4b. As can be seen from the Figure 4b, the maximum sliding speed of the sliding column is 8 m/s, and the maximum sliding displacement is about 12 mm. This is a linear system of friction, and the sliding distance increases with time. In actual friction experiments, due to the limitation of the length of the striking rod and the constraint of the guide hole, the sliding displacement of the upper sliding column generally does not exceed 2.5 mm.

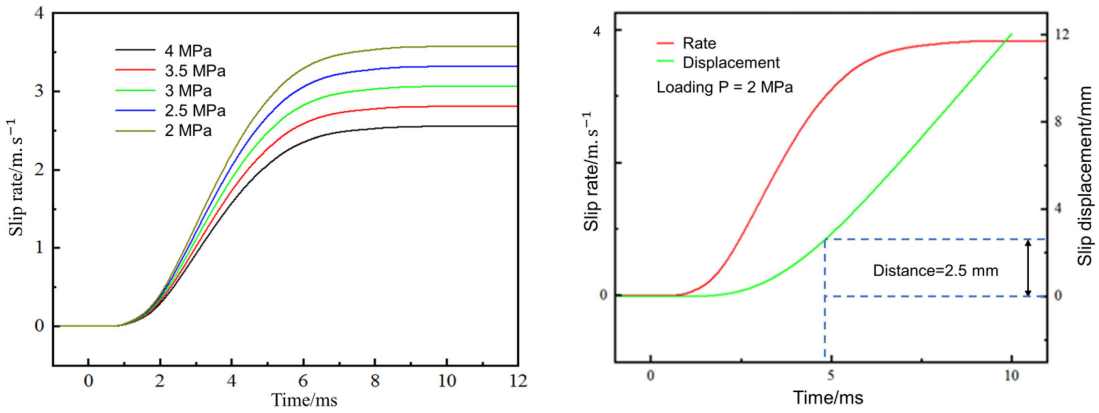

Figure 4. Slip rate and friction displacement curve of the upper sliding column.

2.2. Numerical Simulation

2.2.1. Modeling

The macro simulation physical model of friction ignition experiment is shown in Figure 5. The model is established according to the equal proportion of the size of the experimental device, in which the size of the upper and lower striking columns is the same, which is a cylinder with a diameter of 10 mm and a height of 10 mm. The diameter of HMX-based cast PBX tablets φ the thickness is 1 mm. The vertical downward pressure load is applied on the top of the sliding column on the model, and the pressure load is 2–4 MPa, and the gradient is 0.5 MPa. The friction displacement is applied horizontally, and the displacement load is applied according to the curve. The sliding column is completely fixed.

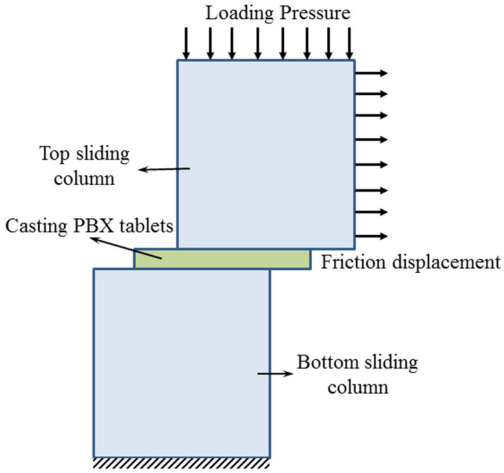

Figure 5. Macroscopic friction model of cast PBX.

The main components of the cast PBX prepared in this paper are HMX/Al powder and HTPB binder. The particle size and gradation of each component need to be considered. The mesoscopic model of cast PBX is built based on the random circle model. The proportion of each particle in the model is closely approximate with that of the cast PBX based on the above Figure 2c. Due to the large number of particles, the mesh and contact action need to be divided, so appropriate simplification is adopted. Some literatures point out a treatment method: small particles and binder matrix are regarded as homogeneous binder system, only the spatial distribution of large particles is considered, and the random spatial coordinates of large particles are given by Matlab function programming. Combined with the electron micrograph of HMX-based PBX explosive sample in Figure 2c, the simplified mesoscopic model is shown in the Figure 6.

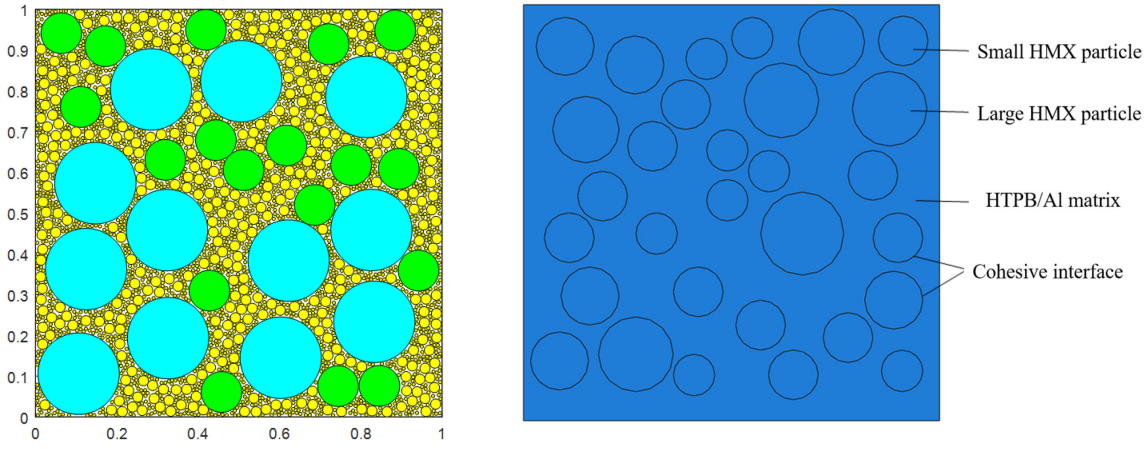

Figure 6. HMX-based cast PBX mesoscopic model: (**a**) random circular mesoscopic model; and (**b**) simplified mesoscopic model by Al and HTPB as a matrix.

A small part of the whole cast PBX tablet was taken and magnified to obtain the mesoscopic model. The friction coefficient f is 0.15. As the friction displacement of the sliding column is relatively small, it can be ignored. Pressure 1 is applied as the loading pressure as shown in Figure 7. The left boundary is fixed horizontally, and there are degrees of freedom in the vertical direction. In the model, the upper sliding column is fixed in the vertical direction, and a fixed displacement is applied to the right. The displacement and amplitude are applied according to the curve. The boundary conditions of the mesoscopic model are shown in Figure 7.

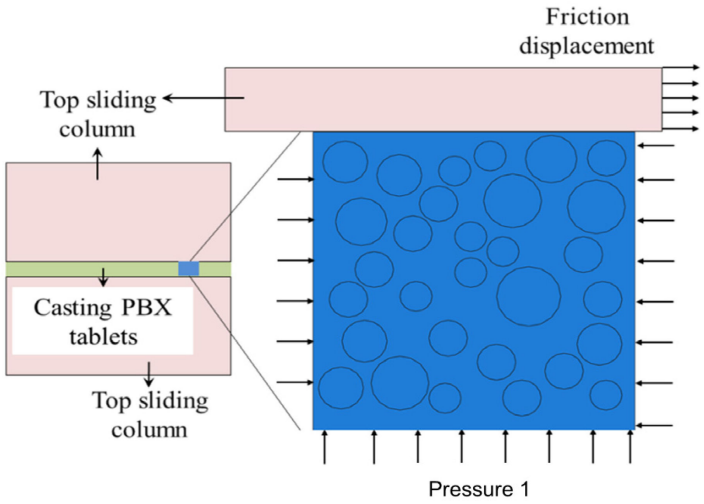

Figure 7. Boundary conditions of mesoscopic model for friction ignition.

2.2.2. Material Model

(1) Viscoelastic material model.

A viscoelastic body is set at any time τ_i have an instantaneous strain $\Delta\varepsilon_i(\tau_i)$, The instantaneous strain $\Delta\varepsilon_i(\tau_i)$, For the stress at any subsequent time t $\sigma(t)$ Impact, in order to $\Delta\sigma_i(t,\tau_i)$ The subscript of Δ indicates that the effect is caused by the i-th strain increment $\Delta\varepsilon_i(\tau_i)$, because the research is linear system, the stress change $\Delta\sigma_i(t,\tau_i)$ and instantaneous strain increment $\Delta\varepsilon_i(\tau_i)$ Satisfy relationship [33]:

$$\Delta\sigma_i(t,\tau_i) = E(t,\tau_i)\,\Delta\varepsilon_i(\tau_i) \tag{4}$$

Before time t, if the instantaneous strain increment $\Delta\varepsilon_i(\tau_i)$ is more than one (i = 1, 2, 3, ⋯, n), and each $\Delta\varepsilon_i$ has no influence on each other. According to the principle of Boltzmann superposition, there are:

$$\sigma(t) = \sum_{i=1}^{n}\Delta\sigma_i(t,\tau_i) = \sum_{i=1}^{n}E(t,\tau_i)\,\Delta\varepsilon_i(\tau_i) \tag{5}$$

When the instantaneous strain is continuous, it becomes $\varepsilon(\tau)$, $(n\to\infty)$, The continuous strain can be obtained $\varepsilon(\tau)$, The expression of stress response is as follows:

$$\sigma(t) = \int_{-\infty}^{t}E(t,\tau)d\varepsilon(\tau) = \int_{-\infty}^{t}E(t,\tau)\frac{\partial\varepsilon}{\partial\tau}d\tau \tag{6}$$

$$E(t,\tau) = 2(1+\nu)\,G(t,\tau) \tag{7}$$

In calculating the curve of relaxation modulus, the stress and strain at different relaxation times need to be measured. According to the integral formula, a method is given in document [34,35]. The exponential series fitting formula is used. The equation is as follows:

$$G(t) = G_\infty + \sum_{i=1}^{n}G_i e^{\frac{-t}{\tau_i^G}} = G_0\left(1-\sum_{i=1}^{n}g_i^P e^{\frac{-t}{\tau_i^G}}\right) \tag{8}$$

$$g_R(t) = 1-\sum_{i=1}^{n}g_i^P e^{\frac{-t}{\tau_i^G}} \tag{9}$$

where $G_0 = G_\infty + \sum_{i=1}^{n}G_i$ is the instantaneous relaxation shear modulus, G_∞ is the steady-state shear modulus, $g_R(t) = G_R(t)/G_0$ is the dimensionless relaxation shear modu-

lus, $g_i^P = G_i/G_0$ is relative modulus of the i-th term. The softening effect of temperature on materials is usually described by Williams-Landel-Ferry (WFL) time-temperature equivalent equation:

$$\tau_i^G = \int_0^t \frac{d\,t'}{a(\theta(\,t'))} \tag{10}$$

$$-\lg(a(\theta(\,t'))) = \frac{\alpha(T - T_{ref})}{\beta + T - T_{ref}} \tag{11}$$

where a is the time temperature transfer function, α and β is constant, T_{ref} is the reference temperature, τ_i^G is the relaxation time. Mechanical and thermal parameters of cast PBX and HTPB/Al matrix are shown in Tables 3 and 4 respectively. Among the Tables 3 and 4, λ is the thermal conductivity coefficient. In addition, q_m is the heat released by the complete decomposition of the unit mass explosive, and E_a is the activation energy in Table 3.

(2) Elastoplastic material model.

Table 3. Mechanical and thermal parameters of cast PBX [36,37].

τ_1/ms	τ_2/ms	τ_3/ms	τ_4/ms	G_0/MPa	ρ (kg/m^3)	λ (W/m·s)	C_v (J/K·g)	q_m (J/g)
7.5×10^{-7}	7.5×10^{-6}	7.5×10^{-7}	7.5×10^{-7}	675.77	1790	0.2	1500	1155
g_1	**g_2**	**g_3**	**g_4**	**υ**	**E_a (J/mol)**	**Z/s^{-1}**	**α**	**β/K**
0.698	0.172	0.1237	0.0063	0.3	2.2×10^5	1.81×10^{19}	−10	107.54

Table 4. Mechanical and thermal parameters of HTPB/Al matrix [15,37,38].

τ_1/ms	τ_3/ms	τ_3/ms	τ_4/ms	τ_5/ms	τ_6/ms	G_0/MPa	ρ (kg/m^3)	λ (W/m·s)	C_v (J/K·g)
1.04×10^{-7}	2.1×10^{-5}	1.66×10^{-3}	0.0105	0.05	0.21	109.53	1400	0.2	1419
g_1	**g_2**	**g_3**	**g_4**	**g_5**	**g_6**	**υ**	**α**	**β/K**	
33	30	25	13	8	6	0.45	−15	102	

Compared with HTPB bonding system, HMX crystal particles has higher hardness and modulus, so it is elastic-plastic. Mechanical and thermal parameters of HMX are shown in Table 5. The constitutive model is as follows:

$$\sigma = \begin{cases} E\varepsilon & \varepsilon \le \varepsilon_0 \\ \sigma_0 + E_t(\varepsilon - \varepsilon_0) & \varepsilon > \varepsilon_0 \end{cases} \tag{12}$$

where E is Young modulus, σ_0 is the yield stress, E_t is plastic hardening rate. The material of upper sliding column and lower sliding column is special steel, the material model is same as HMX crystal particles. Material parameters of sliding column are shown in Table 6. Among Tables 5 and 6, Z is pre-exponential factor, and C_v is the specific heat capacity, respectively.

Table 5. Mechanical and thermal parameters of HMX crystal particles [39,40].

E	υ	σ_0/MPa	E_t/MPa	E_a (J/mol)	Z/s^{-1}	q_m (J/g)	ρ (kg/m^3)	λ (W/m·s)	C_v (J/g·K)
13.3×10^3	0.3	260	5.7×10^3	2.2×10^5	1.81×10^{19}	2100	1865	0.456	1190

Table 6. Material parameters of sliding column [40].

E	υ	σ_0/MPa	ρ (kg/m^3)	λ (W/m·s)	C_v (J/K·g)
2.1×10^5	0.3	1.83×10^3	7800	50	460

2.2.3. Interface Model

(1) Cohesive model.

In the micromechanical analysis, the interface between the binder and explosive plays an important role in the micromechanical properties and thermal response of PBX. On the one hand, the debonding of particles and binder at the interface will cause the mechanical damage of PBX. On the other hand, friction between the debonding explosive particles and the binder will form a high temperature concentration area, which may produce local hot spots. In the existing literature, a cohesive model is used to simulate the debonding phenomenon at the interface, which can better describe the debonding phenomenon between explosive particles and binder, as shown in Figure 8.

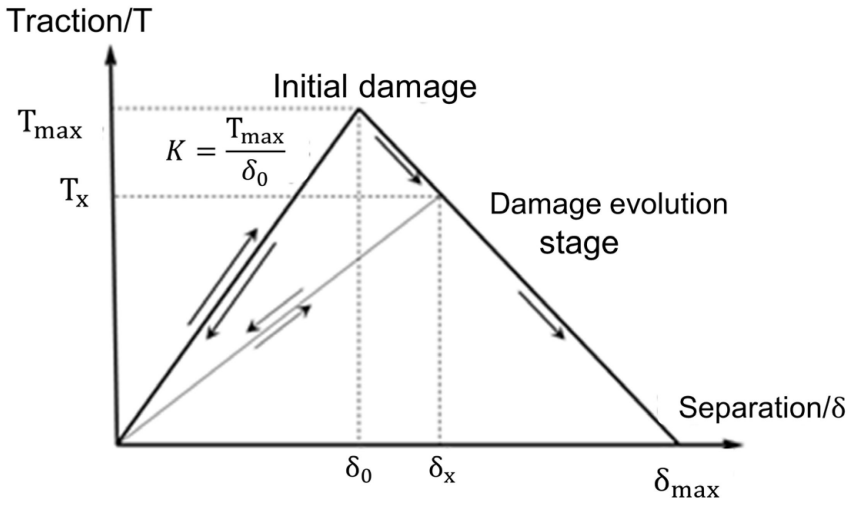

Figure 8. Bilinear cohesive zone model.

In the model, T_{max} is the maximum traction force allowed; δ_0 is the separation amount of the interface during the initial damage, K is the stiffness matrix, $K = \frac{T_{max}}{\delta_0}$. When the traction force $T > T_{max}$, the interface begins to be damaged, and the strength of the model will decrease in the damage evolution stage. When the separation amount $\delta > \delta_{max}$, the model is completely destroyed, and the bonding of the interface fails. Interface parameters of HMX and binder are shown in Table 7. Among the Table 7, μ is the coefficient of friction, and K_c is the heat distribution coefficient between two objects.

Table 7. Interface parameters of HMX crystal particle and binder [15].

K	T_{max}/MPa	δ_0/mm	μ	K_c
792.3	2.91	0.0015	0.3	1.12

The bilinear cohesive unit simulates the mechanical relationship between explosive particles and binder and can analyze the failure between explosive particles and binder. There are three ways to realize cohesive unit in ABAQUS: (a) By inserting a thick cohesive element in the interface layer; (b) Building a thick cohesive element by establishing a thin layer model; (c) Establishing a cohesive contact (Surface-based cohesive behavior) through a contact algorithm.

The first two are constructed by assigning cohesive properties to the units. Each unit is a cohesive mechanical unit. Unfortunately, the cohesive unit in ABAQUS only has mechanical properties and cannot adapt to the thermo-mechanical coupling algorithm. Therefore, the cohesive unit cannot perform thermal and temperature calculations. Calculations can only analyze the mechanical response process, so this paper adopted the last method cohesive contact method to realize the debonding of particles and binder and the friction effect after debonding.

(2) The friction of interface.

After the failure of the cohesive interface, microcracks will be formed, and friction will occur in microcracks. The heat generated by friction is the main reason for the temperature concentration. The heat generated by friction and the distribution law of heat [41] are as follows:

$$Q_f = \mu F_N v \tag{13}$$

$$Q_f = Q_{f1} + Q_{f2} \tag{14}$$

$$K_c = \frac{Q_{f1}}{Q_{f2}} = \sqrt{\frac{\lambda_1 C_{v1} \rho_1}{\lambda_2 C_{v2} \rho_2}} \tag{15}$$

where, Q_f is the heat produced by friction, F_N is the normal pressure, v is the slip rate, μ is the coefficient of friction. Q_f can be further divided into two parts, Q_{f1} and Q_{f2} represents the friction heat of two objects: K_c is the heat distribution coefficient between two objects, λ is the heat conductivity, C_v is the specific heat capacity, ρ is density.

2.2.4. Self Heating Reaction Theory and Heat Transfer Equation of Explosives

The ignition process of explosive in low-speed friction can be explained by the hot spot theory, and the hot spot initiation can be described by the thermal initiation equation. Therefore, it is necessary to analyze the internal thermal balance process of explosive. The internal thermal balance equation of explosive is as follows [42].

$$\rho C \frac{\partial T}{\partial \tau} = \lambda \nabla^2 T + \Phi_V \tag{16}$$

where, $\nabla^2 T$ can be regarded as the inflow heat from the outside; λ is thermal conductivity coefficient and Φ_V is the intensity of internal heat source. The intensity of internal heat source Φ_V is determined by the exothermic intensity of explosive reaction. The thermal decomposition process of explosives is usually expressed as the rate by the first order Arrhenius equation. The total reaction heat per unit volume per unit time of explosives is as follows:

$$\Phi_V = Q_V = \rho q_m c^n k = \rho q_m Z \exp(-\frac{E_a}{RT}) \tag{17}$$

In this paper, the heat-generation subroutine HETVAL is written to realize the heat generation in the thermal decomposition process of explosives. In the actual decomposition process, it is necessary to consider the initial decomposition temperature of explosives. In this paper, the initial decomposition temperature is 554 K. When the temperature of the elemental particles of the explosive is greater than the initial decomposition temperature T_S (554 K), the thermal decomposition reaction of the explosive will be triggered. At lower temperatures, the thermal decomposition rate is lower, and the chemical heat generated is lower. During this process, the frictional heat of microcracks is still the main source of internal heat in explosives. If the temperature continues to rise, the reaction rate of the explosive accelerates, and the heat of chemical reaction becomes the main source of internal heat. Due to the rapid thermal decomposition process of cast PBX, the instantaneous heat flow generated will cause a sharp increase in temperature, which can be considered as the ignition response of the explosive under external stimulus.

3. Results and Discussion

3.1. Response Analysis of PBX Tablet Simulation

3.1.1. Analysis of Tablet Deformation Process

The deformation process and Mises stress nephogram of cast PBX tablet under 3 MPa loading pressure are shown in Figure 9. It can be seen that the casting PBX tablet is first pressed by the hydraulic press. With the sliding of the upper sliding column, the stress

begins to concentrate. The Mises stress of the concentrated unit is much greater than that of the hydraulic press. The maximum Misses stress values at 1 ms, 1.5 ms, 2.5 ms, 4 ms, 6 ms, and 10 ms are 0.32 MPa, 8.93 MPa, 15.64 MPa, 32 MPa, 50.34 MPa, and 55.33 MPa, respectively. As time goes on, the Misses stress at the interface gradually increases. At 2.5 ms, the tablet begins to deform, and the stress-concentration area is the most obvious. Combined with the displacement curve of the upper sliding column, the sliding speed is the fastest. At 4 ms, the deformation of the tablet is intensified, but no distortion occurs. Therefore, the stress concentration area is still in the center of the tablet. With the movement of the upper sliding column, the tablet began to deform. At 6 ms, the tablet was slightly distorted, and the stress concentration area diffused due to the distortion. At 10 ms, the tablet was seriously deformed.

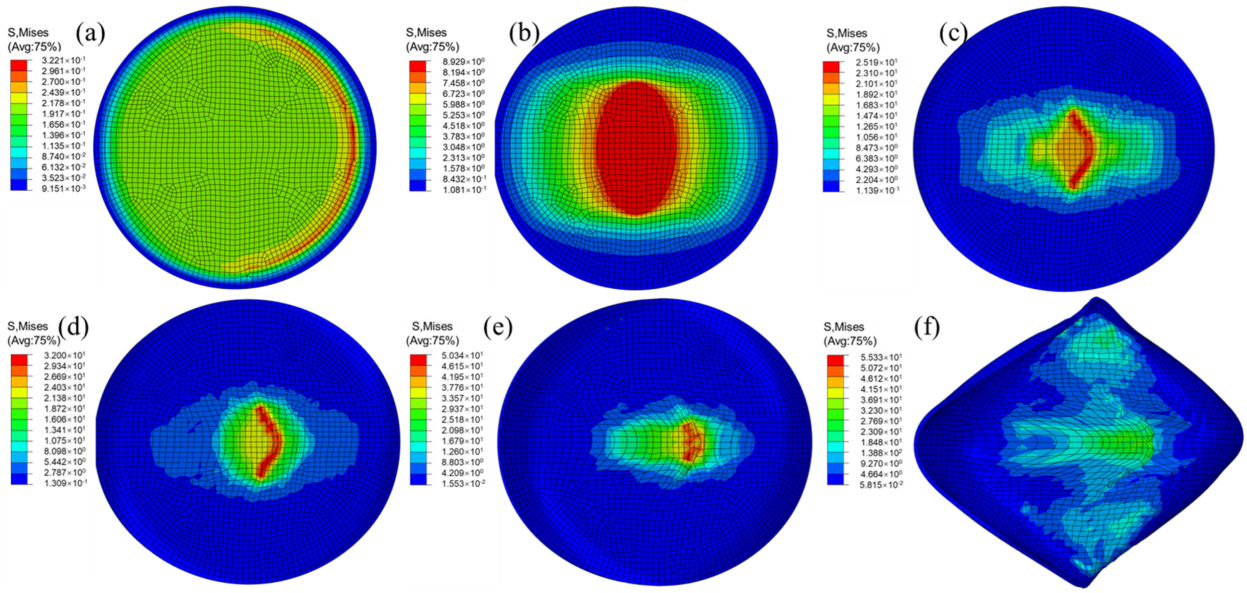

Figure 9. Nephogram of Misses stress and friction deformation of cast PBX tablet: (**a**) t = 1 ms; (**b**) t = 1.5 ms; (**c**) t = 2.5 ms; (**d**) t = 4 ms; (**e**) t = 6 ms; and (**f**) t = 10 ms.

3.1.2. Effect of Loading Pressure on Tablets

Under different hydraulic conditions, the stress and temperature rise of the tablet under friction are also different. The hydraulic pressure of 2 MPa, 2.5 MPa, 3 MPa, 3.5 MPa and 4 MPa is applied, respectively, and the displacement amplitude under the corresponding hydraulic pressure is applied. The stress component (S22) and temperature rise of the central layer unit (Unit No. 1924) of the tablet under different hydraulic pressures are analyzed. The Figure 10 shows the stress component of S22 under hydraulic pressure. With the increase of hydraulic pressure, the stress also increases. The maximum stress under different pressures is 61 MPa, 78 MPa, 87 MPa, 88 MPa and 92 MPa. The figure shows the maximum temperature rise inside the tablet under different hydraulic pressures. The maximum temperature rises under 2–4 MPa hydraulic pressure are 34 °C, 47 °C, 54 °C, 50 °C and 55 °C, respectively. It can be seen that the temperature rise gradually increases with the increase of pressure, but the overall temperature rise is not high.

Through the simulation of friction sensitivity experiment, the influence of pressure on the temperature rise of tablets was analyzed. The simulation results show that the pressure has a great influence on the temperature rise of tablets. When the pressure is low, there is no large area of temperature rise concentration area. With the increase of pressure, the temperature concentration area begins to appear. The concentration area further moves and gradually shrinks, and the maximum temperature rise increases with the increase of pressure. The external friction can make the local temperature of the tablet rise, but it can't

continue. The overall temperature rises are not able to make the explosive ignite, so we need to further consider the ignition mechanism from the micro level.

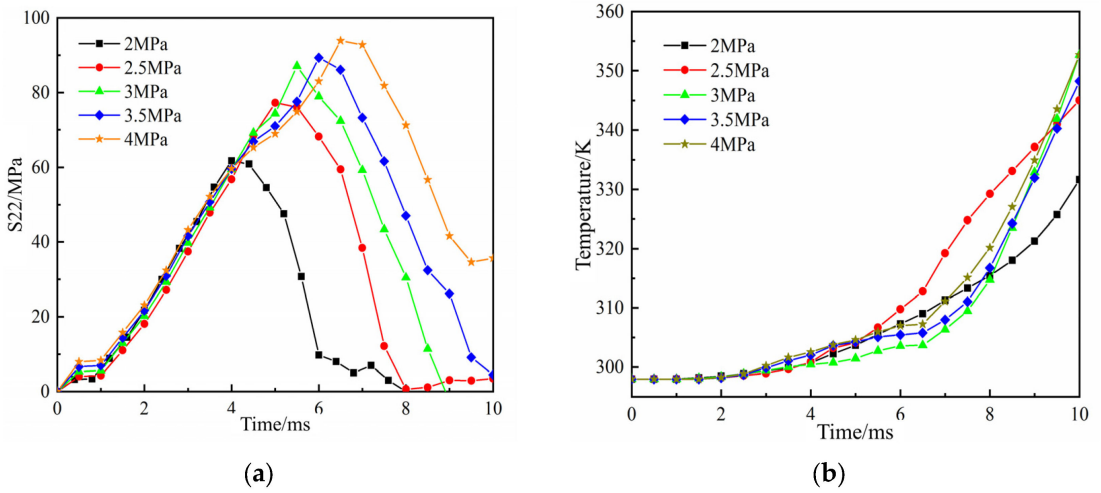

Figure 10. (**a**) Stress components of tablet unit under different hydraulic pressures; and (**b**) temperature rise of tablet unit under different hydraulic pressures.

3.2. Response Analysis of Tablet Mesoscopic Model

3.2.1. Analysis of Micro Ignition Response and Critical Loading Pressure

In order to understand the meso view of the fire process under the action of friction, take the temperature rise cloud diagram of the PBX mesoscopic model under 3.5 MPa and 4 MPa hydraulic pressure to analyze the temperature rise and ignition process are shown in Figure 11. Under 3.5 MPa hydraulic pressure, no explosive particles ignite. Under a loading pressure of 3.5 MPa, the maximum temperature values at 0.75 ms, 2.5 ms, 5 ms, 7 ms, 9 ms, and 10 ms are 298 K, 306 K, 453 K, 579 K, 425 K, and 396 K, respectively. At 0.25 ms, the friction heat at the bottom of the tablet is the main factor affecting the temperature rise. At 7 ms, it can be seen that the heat generated by the bottom friction has almost begun to diffuse into the HMX crystal particles. Due to the interface, the heat conductivity is small, and the heat diffusion is slow. The entire friction process ends at 10 ms, and the heat spreads to the entire explosive area. However, because the temperature accumulation is not obvious enough, and the friction generates little heat, the whole does not ignite.

Figure 11b shows the temperature rise under 4 MPa hydraulic pressure. Under a loading pressure of 4 MPa, the maximum temperature values at 0.75 ms, 2.5 ms, 5 ms, 5.5 ms are 299 K, 355 K, 1253 K, 1630 K. At 5.75 ms and 6 ms, the temperature rose sharply, and ignition occurred. During the sliding process, the distance increases, and the temperature hot spots gradually increase, especially the temperature at the interface between the sliding column and the tablet gradually rises. The temperature rise inside the tablet is mainly concentrated at the interface. The temperature of HTPB at the interface is higher than that of HMX crystal particles. However, as the temperature of HMX rises, the heat-generation subroutine begins. At this time, the self-heating reaction of HMX crystal particles generates a lot of heat, which breaks the original thermal equilibrium state, and the temperature rises sharply. This process can be considered as the process of ignition of HXM particles. It can be seen from the figure that the first smaller temperature rise area starts at 0.25 ms; the local temperature rise points increase with time, and the maximum temperature gradually becomes larger. At 5.5 ms, the temperature distribution cloud map before the critical ignition, the highest the temperature zone is distributed at the microcrack interface. At this time, the corresponding instantaneous temperatures of the matrix and particles are 1654 K and 619 K, respectively. At 5.75 ms, it can be seen that the color of the HMX crystal particles has deepened, indicating that the temperature has risen sharply, and ignition has occurred.

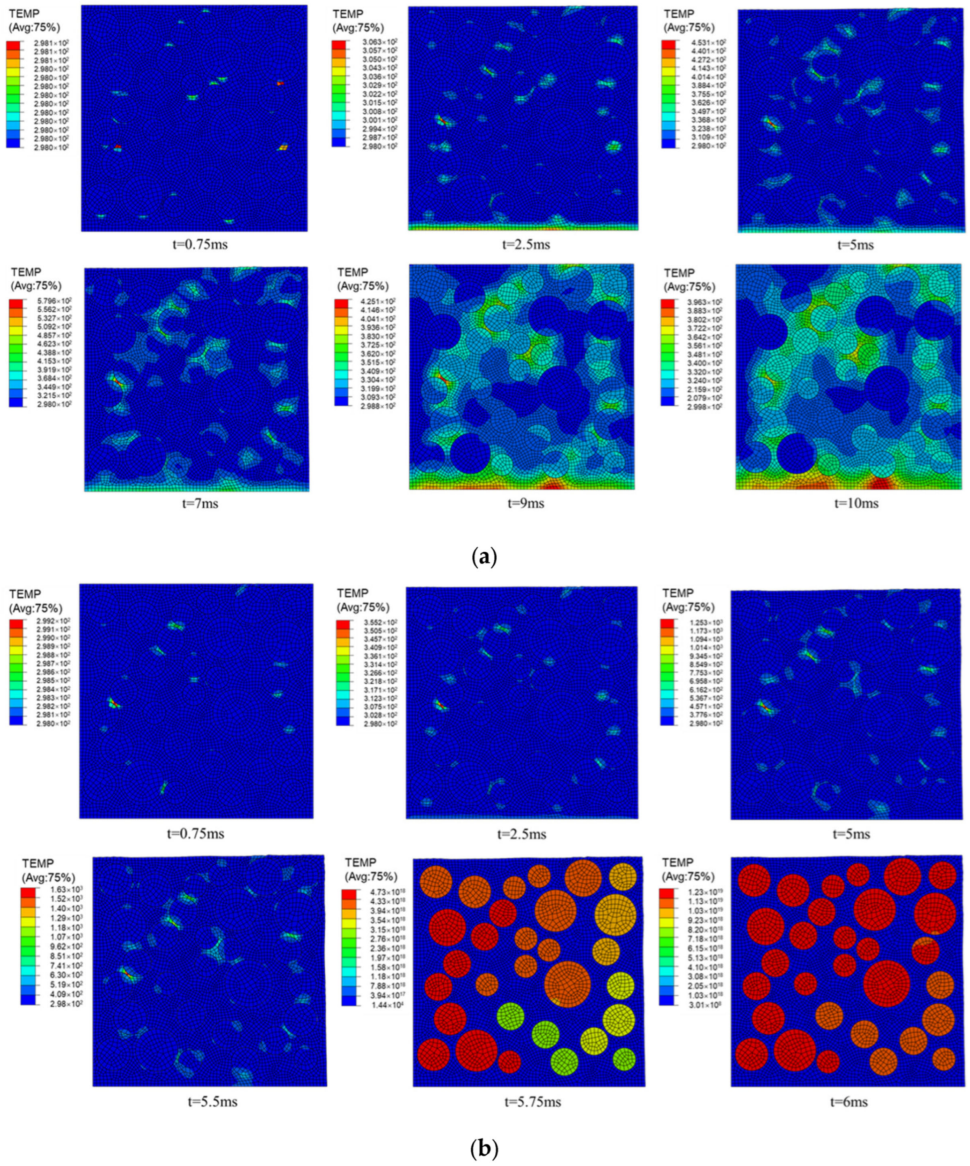

Figure 11. (**a**) Meso-level temperature rise cloud diagram at a loading pressure of 3.5 MPa; (**b**) meso-level temperature rise cloud diagram under a loading pressure of 4 MPa.

The stress distribution inside the PBX tablet is obtained through macro simulation. The tablet under different hydraulic pressures will generate different internal stresses. The stress component at the stress concentration area of the tablet is taken as the boundary load condition of the mesoscopic model, and the stress distribution and the ignition state of the mesoscopic model are analyzed. In order to control irrelevant variables, select the same unit under different pressures for analysis. Figure 12 shows the temperature rise curves of HMX crystal particles under different hydraulic pressures. It can be seen from the figure that with the increase of hydraulic pressure, the maximum temperature rise of HMX crystal particles gradually increases. When the hydraulic pressure is 4 MPa, the temperature of HMX crystal particles rises faster and the heat subroutine is generated. Therefore, it can be judged that the HMX crystal particles are ignited under the hydraulic pressure of 4 MPa. Point A (5.5 ms, 619 K) is the inflection point of temperature rise of explosive particles under 4 MPa hydraulic pressure. The abscissa reflects the time of ignition, and the ordinate is the temperature at the time of ignition. Therefore, it can be judged that the critical ignition hydraulic pressure is between 3.5 MPa and 4 MPa.

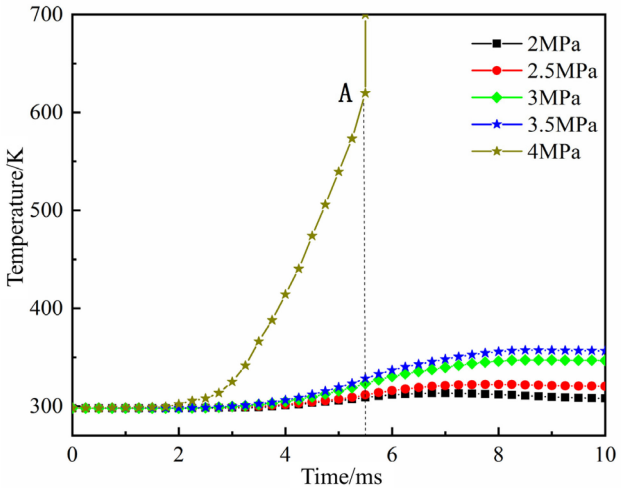

Figure 12. Temperature rises curve of mesoscopic model under different loading pressures.

3.2.2. Influence of Cohesive Interface Friction Coefficient on Ignition

The friction between the HMX crystal particles and the HTPB/Al matrix interface in the cast PBX is the main cause of ignition. At this time, the tablet is subjected to normal stress on the one hand, and frictional shear force on the other hand, under the combined action of pressure and shear force. The stress generated at the interface is relatively concentrated, by adjusting the friction coefficient μ at the cohesive interface to 0.22, 0.27, 0.37 and 0.42, respectively, and the pressure load is set to the minimum ignition pressure 4 MPa to analyze the effect of friction coefficient on ignition.

Figure 13 shows the temperature-rise curves of μ explosive particles with different interfacial friction coefficients. It can be seen from the figure that when the friction coefficient is less than 0.22, no ignition occurs. Where A, B, C, and D are the temperature inflection points when the friction coefficient is 0.27, 0.32, 0.37, 0.42, and the coordinates are A (6.5 ms, 671 K), B (5.5 ms, 620 K), C (5 ms, 704 K), D (4.5 ms, 675.5 K). The abscissa reflects the initial ignition time, and the ordinate reflects the ignition temperature. From the change of the abscissa, it can be judged that the ignition start time shortens with the increase of the friction coefficient. From the change of the ordinate, it can be seen that the friction coefficient has little effect on the initial ignition temperature.

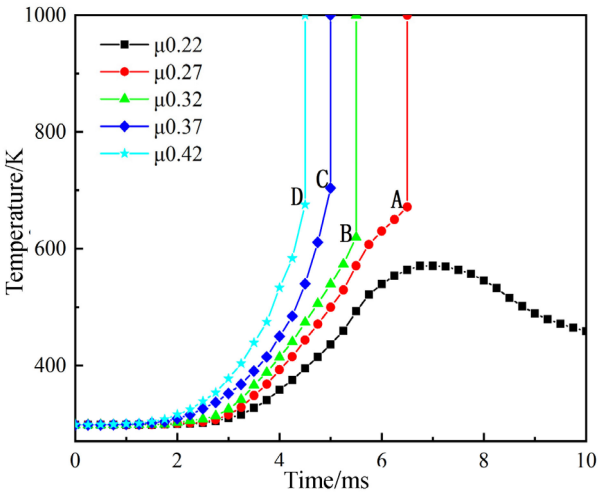

Figure 13. The influence of external friction coefficient on the temperature rise of cast PBX.

The coefficient of friction between the particle and the matrix only affects the ignition time, but has little effect on the ignition temperature. It may be due to the increase in

the friction coefficient and the increase in the resistance of the interface slippage, which reduces the sliding displacement, resulting in friction at the interface. The total heat is relatively constant, and the temperature change is relatively small when the total heat is relatively constant.

3.2.3. The Influence of Friction Coefficient between Slide Column and Tablet on Ignition

In the friction-ignition experiment of the cast PBX tablets, the friction between the tablet and the spool generated higher heat. As mentioned above, the maximum temperature rises of HMX crystal particles under the pressure of 2–4 MPa are 49 °C, 62.2 °C, 72.6 °C and 75.6 °C respectively. The main reason why the cast PBX tablet is ignited by impact is the frictional heat of microcracks at the interface between the particles and the substrate. However, in addition to the internal friction of the tablet under the action of friction, the frictional heat between the tablet and the spool cannot be ignored. Based on this analysis of the influence of external friction on the ignition of the PBX, the friction coefficient f was set to 0.05, 0.25, 0.35, 0.45. The friction coefficient f was set to 0.15 in the previous paragraph. The temperature rises under different friction coefficients under 3.5 MPa and 4 MPa hydraulic pressure were analyzed, as shown in Figure 14.

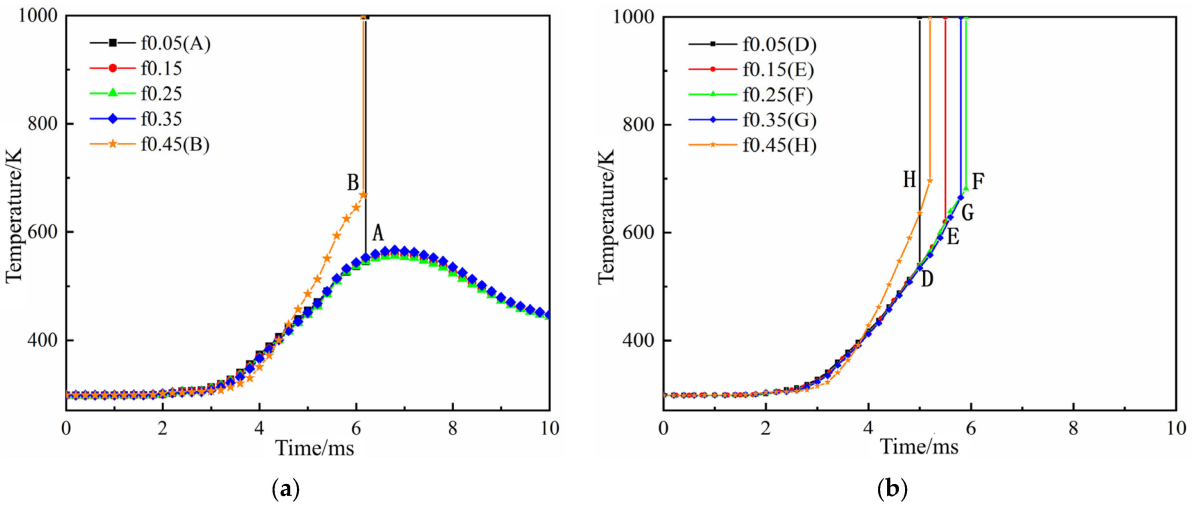

Figure 14. (**a**) The influence of external friction coefficient f on the temperature rise of cast PBX under 3.5 MPa loading pressure; and (**b**) the influence of external friction coefficient f on the temperature rise of cast PBX under 4 MPa loading pressure.

Figure 14a shows the temperature rise curve under 3.5 MPa hydraulic pressure. It can be seen that when the friction coefficient f = 0.05, 0.45, the explosive ignites. But when f = 0.15, 0.25, 0.35, no ignition occurs. The temperature rise curves in the ignition area basically coincide, and the friction coefficient has little effect on the temperature rise of explosive particles. From the analysis of the ignition area, A (6.2 ms, 545 K) and B (6.15 ms, 668 K) are f = 0.05 and 0.45, respectively. The turning point of temperature rise, point A, is suddenly ignited from the original temperature rise, and the ignition does not conform to the general temperature-rise law. It can be judged that the explosive particles of this unit are ignited due to the explosion of other explosive particles, and point B is caused by internal interface friction. The concentrated heat flow triggers the self-heating reaction of the explosive and ignites. Through the above analysis, it can be considered that the friction coefficient f has an effect on the ignition of the cast PBX. However, it does not directly affect the friction heat to affect the ignition of the explosive but affects the ignition by affecting the internal microcrack mechanical behavior.

Figure 14b shows the temperature rise curve at 4 MPa hydraulic pressure, regardless of the friction coefficient, the particles all ignite. Among them, D (5 ms, 539 K), E (5.5 ms, 620 K), F (5.8 ms, 681.5 K), G (5.8 ms, 665 K), H (5.2 ms, 696 K) are the temperature rise

turning points corresponding to the friction coefficient. The temperature at the transition point of the temperature rise at point D is 539 K, which is less than the thermal decomposition starting temperature of 554 K. It can be judged that the explosive at this point was not ignited due to crack friction but was smashed. From the coordinates of points E, F, G and H, it is difficult to determine the ignition law. When f is 0.05–0.35, the temperature-rise curves basically overlap, and it can be considered that the friction coefficient has no effect on the temperature rise but has an effect on the ignition.

4. Conclusions

The critical loading pressure of cast PBX tablet was obtained by friction ignition experiment, and the device was designed to analyze the actual friction rate of the tablet. Then, based on the thermal–mechanical coupling algorithm, the friction ignition process of cast PBX was numerically simulated at the macro and micro scale. The critical conditions of the friction ignition of cast PBX were analyzed by numerical models at different scales. The results of the numerical simulations were consistent with the experimental results, which shows that the numerical simulation is feasible. The main conclusions are as follows:

(1) Friction-ignition experiments were conducted on the HMX-based cast PBX at a 90° swing angle, and the critical ignition loading pressure of 3.7 MPa was determined by the Bruceton method for frictional sensitivity test;
(2) The stress distribution and temperature distribution of the cast PBX tablet under external friction can be obtained by the macro-numerical simulation. It is difficult to draw the conclusion of ignition only by analyzing the whole friction temperature-rise process of the tablet from macro scale;
(3) Based on the morphology characterization results and mesoscopic model simulation of the cast PBX tablets, the temperature rises of HXM particles in PBX tablets under different hydraulic pressures were analyzed, and the ignition loading pressure was determined by ignition criterion. The critical ignition loading pressures determined in this paper is between 3.5 MPa and 4 MPa, which are basically consistent with the experimental critical ignition pressure of 3.7 MPa. The results of the critical ignition loading pressure by numerical simulation were in good agreement with those of the experimental test;
(4) The effects of the cohesive interface friction coefficient μ on the friction ignition of the cast PBX tablet were analyzed. The results showed that the effects of the friction coefficient μ on ignition of cast PBX tablet are obvious. When μ the larger the size of HMX crystal particles, the greater the temperature rise and the greater the possibility of ignition. At the same time, the influences of the friction coefficient f between the slide column and tablet on ignition were analyzed. The results showed that friction coefficient f has an influence on ignition response. The influence does not affect the ignition process by increasing friction heat but can adjusts the ignition result by changing the mechanical conditions inside the cast PBX tablet.

Author Contributions: Conceptualization, J.Y.; methodology, J.Y.; validation, H.P., T.X. and J.L.; formal analysis, W.Z.; data curation, J.Y.; writing—original draft preparation, J.Y. and T.X.; writing—review and editing, J.Y. and Y.Q.; visualization, H.S. and Y.L. All authors have read and agreed to the published version of the manuscript.

Funding: This research was funded by Robust Munitions Center, CAEP (No. RMC2014B03), the Bottleneck Technology and JCJQ Foundation (No. 20210579) and Special Projects of Energetic Materials (No. 20221206).

Data Availability Statement: The data presented in this study are openly available.

Conflicts of Interest: The authors declare no conflict of interest.

Nomenclature

PBX	Polymer-Bonded Explosive
HMX	Cyclotetramethylene tetranitramine
HTPB	Hydroxy terminated polybutadiene
DOA	Dioctyl adipate
TDI	Toluene diisocyanate
τ_i	Time
G_0	Instantaneous relaxation shear modulus
ρ	Density
λ	Heat conductivity
C_v	Specific heat capacity
q_m	Heat released by the complete decomposition of the unit mass explosive
g_i	Relative modulus of the i-th term
υ	Poisson's ratio
E	Young modulus
E_t	Plastic hardening rate
E_a	Activation energy
σ_0	Yield stress
A	Minimum hydraulic pressure loaded by friction sensitivity instrument for initiation
B	Set loading pressure interval
Z	Pre-exponential factor
α	Constant
β	Constant
K	Stiffness matrix
T_{max}	Maximum traction force allowed
δ_0	Separation amount of the interface during the initial damage
μ	Coefficient of friction
K_c	Heat distribution coefficient between two objects

References

1. Gwak, M.-C.; Jung, T.-Y.; Yoh, J.J.-I. Friction-induced ignition modeling of energetic materials. *J. Mech. Sci. Technol.* **2009**, *23*, 1779–1787. [CrossRef]
2. Sun, B.P.; Duan, Z.P.; Pi, A.G.; Ou, Z.C.; Huang, F.L. Approximate analysis on temperature rise in charge explosive during projectile penetration. *Explos. Shock. Waves* **2012**, *32*, 225–230.
3. Deng, C.; Shen, C.Y.; Fan, X.; Xiang, Y. Test on the Friction Sensitivity of PBX Tablet. *Chin. J. Explos. Propellants* **2012**, *35*, 22–24.
4. Charlery, R.; Saulot, A.; Daly, N.; Berthier, Y. Tribological conditions leading to ignition phenomena of energetic materials. In Proceedings of the Leeds Lyon Symposium on Tribology and Tribochemistry Forum, Lyon, France, 4–6 September 2013.
5. Dai, X.G.; Zhong, M.; Deng, C.; Zheng, X.; Wen, Y.S.; Huang, F.L. Reaction Characteristics of PBX Tablet in Friction Sensitivity Test. *Chin. J. Energ. Mater.* **2015**, *23*, 5.
6. Zeman, S.; Jungová, M. Sensitivity and performance of energetic materials. *Propellants Explos. Pyrot* **2016**, *41*, 426–451. [CrossRef]
7. Luo, Y.; Liu, Y.; Huang, F.L. Measurement and Modification of Dynamic Friction Coefficient of Pressed Explosive. *Acta Armamentarii* **2017**, *38*, 1926–1932.
8. Dienes, J.K. Frictional hot-spots and propellant sensitivity. *MRS Online Proc. Libr.* **1983**, *24*, 373–381. [CrossRef]
9. Randolph, A.D.; Hatler, L.E.; Popolato, A. Rapid heating-to-ignition of high explosives. I. Friction heating. *Ind. Eng. Chem. Fundam.* **1976**, *15*, 1–6. [CrossRef]
10. Andersen, W.H. Role of the friction coefficient in the frictional heating ignition of explosives. *Propellants Explos. Pyrot.* **1981**, *6*, 17–23. [CrossRef]
11. An, Q.; Zybin, S.V.; Goddard, W.A., III; Jaramillo-Botero, A.; Blanco, M.; Luo, S.N. Elucidation of the dynamics for hot-spot initiation at nonuniform interfaces of highly shocked material. *Phys. Rev.* **2011**, *84*, 220101. [CrossRef]
12. Cai, Y.; Zhao, F.P.; An, Q.; Wu, H.A.; Goddard, W.A.; Luo, S.N. Shock response of single crystal and nanocrystalline pentaerythritol tetranitrate: Implications to hotspot formation in energetic materials. *J. Chem. Phys.* **2013**, *139*, 164704. [CrossRef] [PubMed]
13. Keshavarz, M.H.; Hayati, M.; Ghariban-Lavasani, S.; Zohari, N. Relationship between activation energy of thermolysis and friction sensitivity of cyclic and acyclic nitramines. *Z. Für Anorg. Und Allg. Chem.* **2016**, *642*, 182–188. [CrossRef]
14. Bouma, R.H.B.; van der Heijden, A.E.D.M. The Effect of RDX Crystal Defect Structure on Mechanical Response of a Polymer-Bonded Explosive. *Propellants Explo. Pyrot.* **2016**, *41*, 484–493. [CrossRef]
15. Hu, R.; Prakash, C.; Tomar, V.; Harr, M.; Gunduz, I.D.; Oskay, C. Experimentally-validated mesoscale modeling of the coupled mechanical–thermal response of AP–HTPB energetic material under dynamic loadin. *Int. J. Fract.* **2017**, *203*, 277–298. [CrossRef]

16. Jafari, M.; Keshavarz, M.H.; Joudaki, F.; Mousaviazar, A. A Simple Method for Predicting Friction Sensitivity of Quaternary Ammonium-Based Energetic Ionic Liquids. *Propellants Explos. Pyrot.* **2018**, *43*, 568–573. [CrossRef]
17. Gruau, C.; Picart, D.; Belmas, R.; Bouton, E.; Delmaire-Sizes, F.; Sabatier, J.; Trumel, H. Ignition of a confined high explosive under low velocity impact. *Int. J. Impact Eng.* **2009**, *36*, 537–550. [CrossRef]
18. Wu, Y.Q.; Huang, F.L. A microscopic model for predicting hot-spot ignition of granular energetic crystals in response to drop-weight impacts. *Mech. Mater.* **2011**, *43*, 835–852. [CrossRef]
19. Bennett, J.G.; Haberman, K.S.; Johnson, J.N.; Asay, B.W. A constitutive model for the non-shock ignition and mechanical response of high explosives. *J. Mech. Phys. Solids* **1998**, *46*, 2303–2322. [CrossRef]
20. Xue, H.J.; Wu, Y.Q.; Yang, K.; Wu, Y. Microcrack-and microvoid-related impact damage and ignition responses for HMX-based polymer-bonded explosives at high temperature. *Def. Technol.* **2022**, *18*, 1602–1621. [CrossRef]
21. Bai, Z.X.; Liu, Q.J.; Liu, F.S.; Jiang, C.L. Three-dimensional discrete element method to simulate the ignition and combustion of HMX explosives under hot spots. *Powder Technol.* **2022**, *412*, 118014. [CrossRef]
22. Li, H.T.; Sun, J.; Sui, H.L.; Chai, C.G.; Li, B.H.; Yu, J.X. Influencing mechanisms of a wax layer on the micro-friction behavior of the β-HMX crystal surface. *Energetic Mater. Front.* **2022**, *3*, 248–256. [CrossRef]
23. Yin, Y.; Li, H.T.; Cao, Z.H.; Li, B.H.; Li, Q.S.; He, H.T.; Yu, J.X. Crystallographic orientation dependence on nanoscale friction behavior of energetic β-HMX crystal. *Friction* **2023**, *10*, 1–14. [CrossRef]
24. Duarte, C.A.; Koslowski, M. Hot-spots in polycrystalline β-tetramethylene tetranitramine (β-HMX): The role of plasticity and friction. *J. Mech. Phys. Solids* **2023**, *171*, 105157. [CrossRef]
25. Barua, A.; Kim, S.; Horie, Y.; Zhou, M. Ignition criterion for heterogeneous energetic materials based on hotspot size-temperature threshold. *J. Appl. Phys.* **2013**, *113*, 064906.1–064906.22. [CrossRef]
26. Barua, A.; Kim, S.; Horie, Y.; Min, Z. Computational Analysis of Ignition in Heterogeneous Energetic Materials. *Mater. Sci. Forum* **2014**, *767*, 13–21. [CrossRef]
27. Kim, S.; Barua, A.; Horie, Y.; Min, Z. Ignition probability of polymer-bonded explosives accounting for multiple sources of material stochasticity. *J. Appl. Phys.* **2014**, *115*, 27–33. [CrossRef]
28. Barua, A.; Kim, S.; Horie, Y.; Min, Z. Prediction of Probabilistic Ignition behavior of polymer-bonded explosives from microstructural stochasticity. *J. Appl. Phys.* **2013**, *113*, 537–550. [CrossRef]
29. Keyhani, A.; Horie, Y.; Zhou, M. Relative importance of plasticity and fracture/friction in ignition of polymer-bonded explosives (PBXs). In Proceedings of the 20th Biennial Conference of the APS Topical Group on Shock Compression of Condensed Matter, St. Louis, MO, USA, 14 July 2017.
30. Vadhe, P.P.; Pawar, R.B.; Sinha, R.K.; Asthana, S.N.; Rao, A.S. Cast aluminized explosives. *Combust. Explos. Shock. Waves* **2008**, *44*, 461–477. [CrossRef]
31. Chen, H.T. *QJ 2913-1997. Test Method for Friction Sensitivity of Composite Solid Propellants*; Industry Standard-Aerospace: Beijing, China, 1997.
32. Che, T.Z.; Jiang, W.Q.; Zheng, Z.D.; Xu, Y.F.; Wang, B.L. *QJ 3039-1998. Test Method for Drop Weight Impact Sensitivity of Composite Solid Propellants*; Industry Standard-Aerospace: Beijing, China, 1997.
33. Chen, J.; Zeng, X.G.; Chen, H.Y. *Viscoelastic Mechanics*; Sichuan University Press: Chengdu, China, 2016; pp. 78–88.
34. Mas, E.M.; Clements, B.E.; Blumenthal, B.; Cady, C.M.; Gray, G.T.; Liu, C. A viscoelastic model for PBX binders. *AIP Conf. Proc.* **2002**, *620*, 661–664.
35. Simulia, D.S.; Fallis, A.G. ABAQUS documentation. *Mendeley* **2013**, *53*, 1689–1699.
36. Amirkhizi, A.V.; Isaacs, J.; McGee, J.; Nasser-Nemat, S. An experimentally-based viscoelastic constitutive model for polyurea, including pressure and temperature effects. *Philos. Mag.* **2006**, *86*, 5847–5866. [CrossRef]
37. Tarver, C.M.; Tran, T.D. Thermal decomposition models for HMX-based plastic bonded explosives. *Combust. Flame* **2004**, *137*, 50–62. [CrossRef]
38. Hanson-Parr, D.M.; Parr, T.P. Thermal properties measurements of solid rocket propellant oxidizers and binder materials as a function of temperature. *J. Energ. Mater.* **1999**, *17*, 1–48. [CrossRef]
39. Wu, Y.Q.; Huang, F.L. A micromechanical model for predicting combined damage of particles and interface debonding in PBX explosives. *Mech. Mater.* **2009**, *41*, 27–47.
40. Liu, Q.; Chen, L.; Wu, J.Y.; Wang, C. Two dimensional numerical simulation of shock ignition of PBX explosive mesostructure. *Chin. J. Explos. Propellants* **2011**, *34*, 10–16.
41. Kang, G.; Chen, P.W.; Zeng, Y.L.; Ning, Y.J. A Method of Generating Mesoscopic Models for PBXs with High Particle Volume Fraction. *Chin. J. Energ. Mater.* **2018**, *26*, 772–778.
42. Zhang, X.Z.; Huang, W.; Liu, Q.G. *Heat Transfer*; National Defense Industry Press: Beijing, China, 2011; pp. 9–11.